

# CFD modelling of the interaction between the Surface Boundary Layer and rotor wake

## Comparison of results obtained with different turbulence models and mesh strategies

D. Cabezón<sup>1)</sup>, J. Sanz<sup>1)</sup>, I. Martí<sup>1)</sup>, A. Crespo<sup>2)</sup>

<sup>1)</sup> Wind Energy Department, National Renewable Energy Centre (CENER), Spain

<sup>2)</sup> Departamento de Ingeniería Energética y Fluidomecánica, Escuela Técnica Superior de Ingenieros Industriales, Universidad Politécnica de Madrid (UPM)

e-mail: [dcabezon@cener.com](mailto:dcabezon@cener.com), Tlf: +34914175042, Fax : +34915566300

### Abstract

A simplified CFD wake model based on the actuator disk concept is used to simulate the wind turbine, represented by a disk upon which a distribution of forces, defined as axial momentum sources, are applied on the incoming non-uniform flow. The rotor is supposed to be uniformly loaded, with the exerted forces function of the incident wind speed, the thrust coefficient and the rotor diameter. The model is tested under different parameterizations of turbulence models and validated through experimental measurements downwind of a wind turbine in terms of wind speed deficit and turbulence intensity.

Keywords: actuator disk, thrust coefficient, turbulence modelling

### 1. Introduction

Wind turbine rotor effect has been modelled using several types of approaches [1], from analytical engineering models to 3D CFD full rotor modelling. During the last years and due to the need of modelling the far wake and wind turbines interaction in challenging environments such as complex terrain and offshore, new proposals have arisen through the so-called 'back to the basics' concept.

An elliptical approach based on coupling the actuator disk technique and CFD can make a fair simplification of the rotor without leaving the main essence of its physics. The proposed model is just based on the thrust coefficient (so that the geometry of rotor blades is not considered) and calculates the extraction of momentum from the incoming flow at the rotor face by applying a distribution of forces uniformly loaded over the rotor. Using specific techniques on the actuator disk approach such as the BEM model compared to more simplified approximations just based on the thrust coefficient have demonstrated to have small or even no impact on the axial

evolution of the far wake [2], where wake interaction, turbulence modelling and topographical effects are particularly more relevant.

This paper faces the task of finding an optimum interface modeling between the surface boundary layer meteorology as the bounding environment of wakes and rotor aerodynamics. A sensitivity analysis is made for two relevant topics: firstly, meshing topologies and secondly, the parameterization of isotropic k- $\epsilon$  turbulence model in its standard and realizable versions as well as an additional approach through the anisotropic model RSM (Reynolds Stress Model). The results obtained from the actuator disk technique will be compared to single-rotor wake field measurements [4] in order to observe the prediction accuracy of wind speed deficit and added turbulence intensity. These results could also help to enlighten the starting point for the study of how meshing strategies and the turbulence models parameterization could be adjusted in order to simulate rotor wakes in a more efficient way.

### 2. Sexbierum experiment

The main objective of the Sexbierum experiment consisted of measuring and analyzing wake flow downwind of a three bladed 300 kW wind turbine, with a rotor diameter of 30m and 35m of hub height [4]. For that purpose, a met mast was located 2.8D upstream of the wind turbine and another three met masts downstream, at distances of 2.5D, 5.5D and 8D, in order to characterize the near and far wake as a whole (fig. 1). For the measurement period, the upstream met mast registered at hub height a free stream velocity of 10 m/s and a turbulence intensity of 10%, equivalent to an axial thrust coefficient of  $C_T=0.75$  and a local roughness length of  $z_0=0.0018m$ , respectively. These parameters are used for the definition of the incoming flow at the

entrance of the domain for the simulation of the rotor.

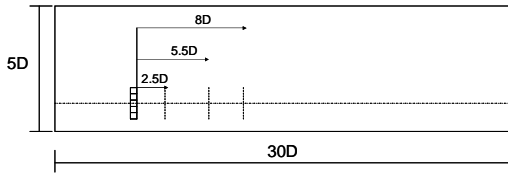


Fig. 1 Location of met masts at the positions downstream of the rotor

### 3. Numerical model

#### 3.1 Surface Boundary Layer modelling

A non-uniform flow is modelled in a computational domain of 30D x 7D x 5D, representing the surface boundary layer (SBL), in which the Monin-Obukhov theory for neutral atmosphere is represented and solved by means of the Reynolds Averaged Navier Stokes equations.

A structured grid was generated with ICFM CFD Hexa (Ansys Inc.) getting a domain of approximately 230,000 hexas. The inlet profiles are defined by the wind speed, turbulent kinetic energy and turbulent dissipation rate profiles, as specified by the Monin-Obukhov theory for the SBL.

The ground was simulated as a wall, through the adaption of the standard wall functions through a link between the turbulent law-of-the-wall modified for mechanical roughness and SBL log-law, based on the roughness length [5].

#### 3.2 Actuator disk model

From the linear momentum theory in its simplest form, it can be derived that the axial force from which the wind turbine extracts the kinetic energy from the incoming air flow, is just a function of the local induction factor or alternatively, from the thrust coefficient for the corresponding upstream wind speed [6][7][8]. The wind turbine is thus considered as an actuator disk upon which a uniform distribution of axial forces, defined as momentum sources, is applied. These local axial forces can be prescribed over the area of rotor disk as:

$$F = \frac{1}{2} \rho \cdot A \cdot C_t \cdot V_{inf}^2$$

where:

- A = rotor diameter (m<sup>2</sup>)
- C<sub>t</sub> =thrust coefficient
- V<sub>inf</sub> =upstream wind speed (m/s)

The local prescribed force is to be applied on a volume of cells defining the rotor in units of force per cubic meter (N/m<sup>3</sup>)

### 4. Grid independence study

From the meshing point of view and considering the structured grid above defined for the simulation of the SBL flow, there is not any previous guideline on the definition of the rotor volume from which the kinetic energy is to be extracted from the incoming flow.

That is why a previous sensitivity analysis should be made in order to estimate the optimum number of cells to be used in the axial and lateral directions. If a rotor disk like the one in figures 2 and 3 is considered, three different tentative spacing can be planned in order to observe the evolution of the wind speed deficit modelled by the actuator disk in the axial and lateral directions.

The vertical distribution of nodes corresponds to the mostly recommended one in the definition of the SBL, with a first grid cell of 1m high and an approximate increasing ratio of 1.12 in the vertical direction, getting around 9-10 nodes below hub height, in order to capture the main velocity gradients in the lowest layer next to the ground.

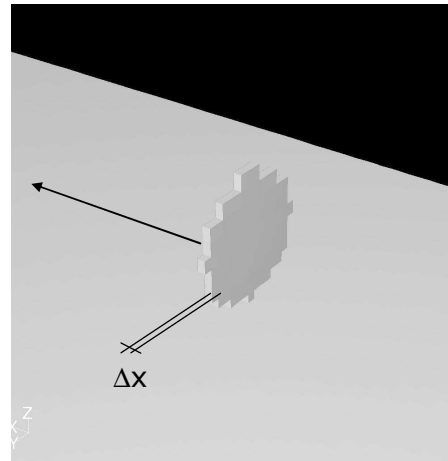


Fig. 2 Actuator disk model. Axial view

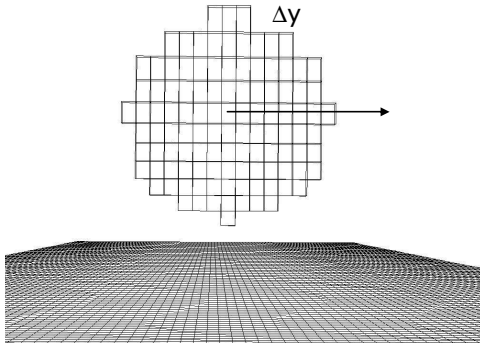


Fig. 3 Actuator disk model. Lateral view

#### 4.1 Grid independence in axial direction

The first grid analysis relies on the axial wind direction and affects to the thickness of the rotor disk to be represented. As it is shown in figure 4, the analysis makes some difference on the evolution of the axial wind speed deficit in the near wake, up to 7D-8D. Above this distance, the deficits are very similar and no relevant difference is appreciated. Taking into account that the near wake is also to be prescribed for this analysis, an axial spacing of 0.06D is used.

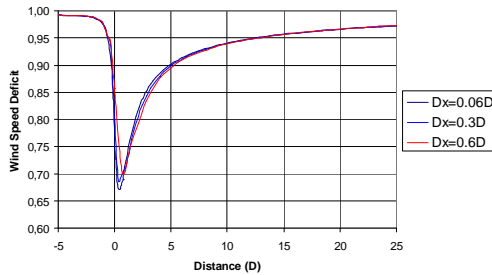


Fig. 4 Grid sensitivity in axial direction

#### 4.2 Independence in lateral direction

The second part of the grid independence analysis refers to the number of control volumes (CV) to be used in the lateral direction of the rotor disk. For that purpose, lateral spacing of 0.06D, 0.16D and 0.3D are used. Figure 5 describes the evolution in the near wake at  $x=2.5D$  of the wind speed deficit along the lateral direction. The results show that for 0.06D and 0.16D the difference is very slight whereas for a spacing of 0.3D the difference is more relevant. For that reason, a spacing of 0.16D, equivalent to 6 lateral nodes as optimum number in the lateral direction.

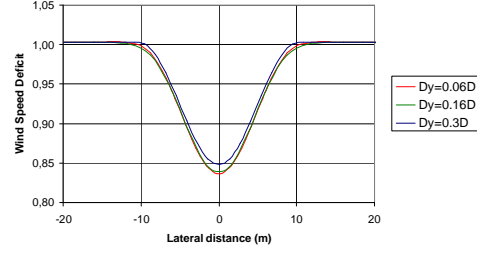


Fig. 5 Grid sensitivity in lateral direction

With this result and the previous one, a number of around 30-40 CVs per rotor disk is found to be the optimum one in order to preserve independence on the results.

### 5. Turbulence modelling

#### 5.1 Isotropic $k\epsilon$ standard

This is the simplest form of the  $k\epsilon$  turbulence models and widely used for its robustness and economy when solving relatively simple flows.

The turbulent kinetic energy  $k$  and dissipation rate  $\epsilon$  are obtained from the following transport equations:

$$\frac{\partial}{\partial t}(\rho k) + \frac{\partial}{\partial x_i}(\rho k u_i) = \frac{\partial}{\partial x_i} \left[ \left( \mu + \frac{\mu_t}{\sigma_k} \right) \frac{\partial k}{\partial x_j} \right] + G_k - \rho \epsilon \quad (1)$$

$$\frac{\partial}{\partial t}(\rho \epsilon) + \frac{\partial}{\partial x_i}(\rho \epsilon u_i) = \frac{\partial}{\partial x_j} \left[ \left( \mu + \frac{\mu_t}{\sigma_\epsilon} \right) \frac{\partial \epsilon}{\partial x_j} \right] + C_{1\epsilon} \frac{\epsilon}{k} G_k - C_{2\epsilon} \rho \frac{\epsilon^2}{k} \quad (2)$$

where  $G_k$  represents the generation of turbulent kinetic energy due to the mean velocity gradients and the turbulent viscosity is computed as follows:

$$\mu_t = \rho C_\mu \frac{k^2}{\epsilon} \quad (3)$$

When applied to the resolution of the SBL [9], it is common practice to make use of its parameterization based on the standard deviations measurements indicated in Panofsky and Dutton [10].

$$C_\mu = 0.033, C_{1\epsilon} = 1.176, C_{2\epsilon} = 1.92, \sigma_k = 1.0, \sigma_\epsilon = 1.3$$

which met the condition of local equilibrium at the wall:

$$\sigma_\epsilon = \frac{\kappa^2}{(C_{2\epsilon} - C_{1\epsilon}) \sqrt{C_\mu}} \quad (4)$$

where  $\kappa$  is the von Karman constant  $\kappa \approx 0.4$ .

The model is likely to be inaccurate for all cases where strong gradients exist in areas

of great curvature, giving an overestimation of the turbulent viscosity.

### 5.2 Isotropic $k\epsilon$ standard. Correction in $\epsilon$ equation

Recent work by El Kasmi and Masson proposed a correction in the  $\epsilon$  equation by increasing locally the turbulent dissipation rate in order to mitigate the excess of turbulent diffusion, improving thus the energy exchange from the larger to the smaller scales [2].

The model is applied in this paper, by correcting the constants such that the hypothesis of equilibrium in the wall (4) is conserved.

### 5.3 Isotropic $k\epsilon$ Realizable

The realizable model proposed by Shih et al. [11], differs from the standard model in two different ways:

First, a new turbulent viscosity formulation involving a variable  $C_\mu$  (5) as a function of the mean strain rate and the turbulence fields in terms of  $k$  and  $\epsilon$ . This new value is computed from:

$$C_\mu = \frac{1}{A_0 + A_s \frac{kU^*}{\epsilon}} \quad (5)$$

$$(18)$$

$$\text{where, } A_0 = 4.04 \quad U^* = \sqrt{S_{ij}S_{ij}}$$

$$A_s = F(S_{ij})$$

Secondly a new transport equation (6) for the dissipation rate  $\epsilon$  is proposed. In the same way, the constant associated to the generation of  $\epsilon$  is affected by the mean strain tensor, making the upper value to be limited according to the equation (7).

$$\frac{\partial}{\partial x_j} (\rho \epsilon u_j) = \frac{\partial}{\partial x_j} \left[ \left( \mu + \frac{\mu_t}{\sigma_\epsilon} \right) \frac{\partial \epsilon}{\partial x_j} \right] + \rho C_{1\epsilon} S \epsilon - \rho C_{2\epsilon} \frac{\epsilon^2}{k + \sqrt{V\epsilon}} \quad (6)$$

$$\text{where, } C_{1\epsilon} = \max \left[ 0.43, \frac{\eta}{\eta + 5} \right] \quad (7)$$

$$\eta = S \frac{k}{\epsilon} \quad S = \sqrt{2S_{ij}S_{ij}}$$

The default model constants are:

$$C_{1\epsilon} = 1.44, C_{2\epsilon} = 1.9, \sigma_k = 1.0, \sigma_\epsilon = 1.2$$

Nevertheless, before using the model for the simulation of the rotor wake, it must be previously calibrated for freestream conditions in order to ensure the equilibrium in the SBL of the inlet profiles with the ground and the turbulence model parameterization along the domain.

Figure 5 shows the axial evolution at hub height of  $C_\mu$  and  $C_{1\epsilon}$  according to (5) and

(7), when the TKE and  $\epsilon$  profiles of the SBL are introduced at the inlet, with the corresponding value of  $C_\mu=0.033$ . The results show for this case that no equilibrium is reached along the domain so that the values of  $C_\mu$  and  $C_{1\epsilon}$  are not conserved, whereas a value  $C_\mu = 0.09$  (default for Standard  $k\epsilon$  model) leads indeed to equilibrium for these parameters. From this result it is concluded that the realizable turbulence model as defined in Fluent 6.3 reaches equilibrium just for  $C_\mu = 0.09$  when the SBL is tried to be simulated through it.

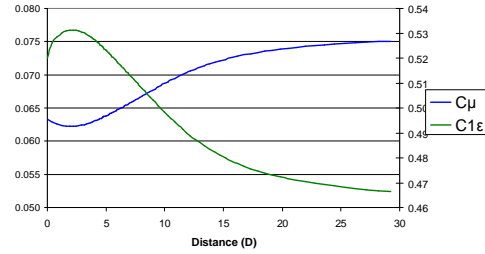


Fig. 5 Axial evolution of  $C_\mu$  and  $C_{1\epsilon}$  along the domain under freestream conditions

Despite of this circumstance, the model has also been tested in order to estimate its accuracy when simulating strong velocity gradients at rotor wakes, but using a different freestream turbulence intensity, conditioned by the value of  $C_\mu=0.09$  in order to get the equilibrium value of  $C_\mu = 0.09$

### 5.4 Anisotropic Reynolds Stress Model (RSM)

Another approach of simulating the turbulence mixing in the wake is to consider the anisotropic resolution of the fluid motion equations, by solving all the terms in the Reynolds Stress Tensor, through the introduction of seven extra equations into the system configuring thus the so-called RSM (Reynolds Stress Model). For this purpose, the  $\overline{u'_i u'_j}$  profiles defined for ABL as indicated by Panofsky [10] are used at the entrance of the domain.

$$\frac{\sigma_x}{u_*} = 2.39 \quad \frac{\sigma_y}{u_*} = 1.92 \quad \frac{\sigma_z}{u_*} = 1.25 \quad (8)$$

Specific description of this model is out of the scope at this point and will be omitted for simplicity.

## 6. Results

Two type of output results were prescribed, in terms of wind speed deficit and turbulence intensity at 2.5D, 5.5D and 8D downstream of the wind turbine.

Figures 6 to 11 describe the lateral evolution of the wake for the different turbulent schemes as a function of the incoming wind direction and its comparison with the measurements at each mast.

### 6.1 Wind speed deficit

The main and primary result of the analysis leads to the underestimation of wind speed deficit made by the standard  $k\epsilon$  turbulence model in its default parameterization. This result, mainly due to the excess of turbulence diffusion in the wake, makes the flow to recover much earlier than expected, getting values of more than 90% in the far wake section in figure 8.

The proposed corrections on the  $k\epsilon$  standard default model show a better agreement with the measurements, specially in the 5.5D and 8D sections.

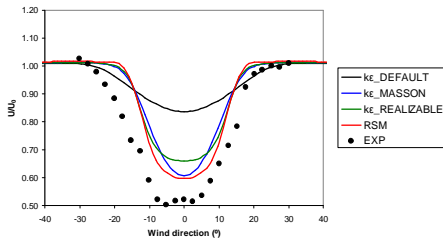


Fig. 6 Wind speed deficit in the average flow direction at a downstream distance of 2.5D

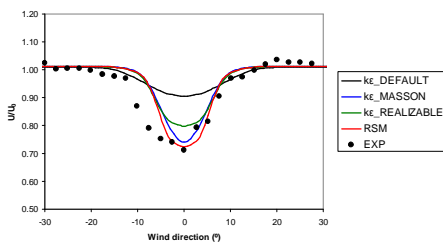


Fig. 7 Wind speed deficit in the average flow direction at a downstream distance of 5.5D

The local increase in the turbulent dissipation rate makes the turbulence mixing to be mitigated so that the recovery of the flow is slower, obtaining more realistic wind speed deficits.

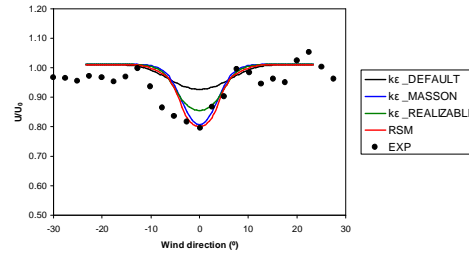


Fig. 8 Wind speed deficit in the average flow direction at a downstream distance of 8D

The anisotropic treatment of the flow through the RSM model gets also very acceptable results, not only in the far wake but also in the near wake, and a more accurate prediction of the wake expansion downstream of the wind turbine.

### 6.2 Turbulence intensity

The results extracted from the isotropic turbulence models for the prescription of the turbulence intensity assumes the hypothesis of isotropy in the wake and anisotropy in the freestream, making the turbulent kinetic energy to be processed on that way. The turbulence intensity extracted from the RSM model, is directly prescribed from the variance of axial wind speed.

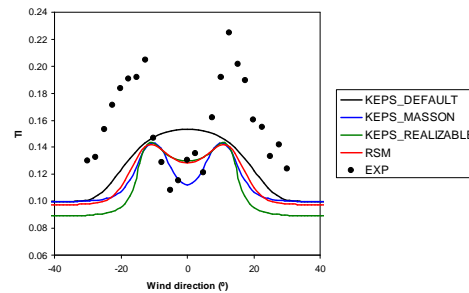


Fig. 9 Turbulence intensity in the average flow direction at a downstream distance of 2.5D

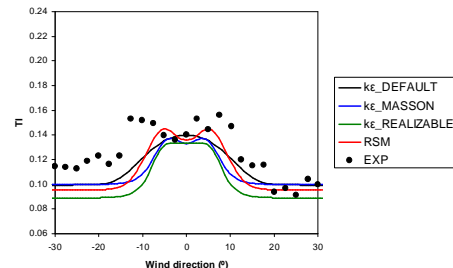


Fig. 10 Turbulence intensity in the average flow direction at a downstream distance of 5.5D

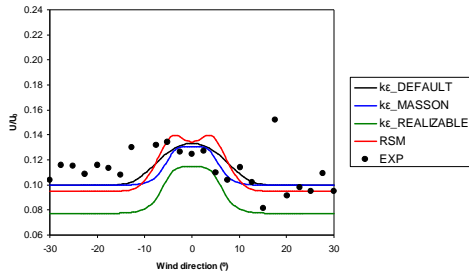


Fig. 11 Turbulence intensity in the average flow direction at a downstream distance of 8D

The results in figures 9 to 11 show that, although all the models underestimate the turbulence intensity in the near wake, the prediction is very acceptable in the two sections located in the far wake, especially in the area near the wake axis. Local corrections on the prognostic equation for  $\epsilon$  as well as the anisotropic RSM make the high shear zones to join into the wake axis in a section further than predicted by the default parameterization, as it observed from the measurements.

## 7. Conclusions

The parameterization of isotropic  $k\epsilon$  turbulence models used by default for the simulation of single rotor wakes in the SBL leads to an underestimation of the wind speed deficit. Local corrections on the  $\epsilon$  equation should be made in order to counteract the excess of turbulent diffusion in the near wake flow produced by the standard  $k\epsilon$  turbulence model. Some of them give very acceptable results in the far wake region where wind turbines are usually placed. Higher order turbulence models such as the anisotropic RSM are also quite promising and offer also accurate predictions of the wind speed deficit in the far wake.

RANS model as described in this paper combined with the actuator disk technique based on linear momentum theory offers in general very acceptable results in the far wake sections and will never be so accurate as space filtering models such the LES models in the prediction of the near wake flow. That is why these economic models based on the actuator disk technique are very acceptable for wind farm analysis applications where the main interest relies on the prediction of the far wake, whereas LES modeling, with accurate predictions of the flow usually for all the sections, are highly recommended for local studies of individual nacelle and

rotor aerodynamics, but with an obvious important increase on the computing effort, not affordable for an operational use.

The analysis carried out on this work constitutes the first stage of the next generation CFD wake models for the simulation of large wind farms in complex terrain and offshore.

## 8. Further work

The results obtained for this analysis corresponds to a stand-alone wind turbine but no conclusion is reached on how these schemes will behave in wind farm environments.

With that purpose, similar validations will be run from wind farm measurements in order to observe how mesoscale effects, such as thermal induction derived from atmospheric stability (especially in offshore conditions) or the different turbulent length scales and microscale effects such as wake merging or terrain interaction, can influence the evolution of the wake.

On the same way, different aspects such as mesh refinement around the shear layer of the wake will also be studied in order to assess its interest.

## REFERENCES

1. Vermeer L.J. et. al., 2003, Wind turbine wake aerodynamics. Prog. Aerosp. Sci. 39, 467-510
2. El Kasmin A., Masson C., An extended  $k\epsilon$  model for turbulent flow through horizontal-axis wind turbines, J. Wind Engineering and Industrial Aerodynamics 96 (2008), 103-122
3. Crespo A., Manuel F., and Hernández J., Numerical modelling of wind turbine wakes. European Community Wind Energy Conference Proceedings, Madrid, September 1990
4. Cleijne J.W., Results of Sexbierum Wind Farm, Report MT-TNO Apeldoorn 92-388, 1992
5. Sanz J., Cabezón D., Martí I., Van Beeck J. et.al Numerical CFD modeling of non-neutral atmospheric boundary layers for offshore wind resource assessment based on Monin-Obukhov theory. Proceedings of the European Wind Energy Conference, March 2008, Brussels (Belgium)
6. Réthoré P., Sørensen N., Zahle F., Bechmann A., Study of the wake turbulence of a CFD actuator disk model compared with a full rotor CFD model, Proceedings of the European Wind Energy Conference 2009, Marseille (France)
7. Politis E., Rados K., et. al., CFD modeling issues of wind turbine wakes under stable atmospheric conditions, Proceedings of the European Wind Energy Conference 2009, Marseille (France)
8. Jimenez A., Crespo A., et. al., Large-eddy simulation of a wind turbine wake, Proceedings of the European Academy of Wind Energy Seminar, October 2007, Pamplona (Spain)

9. Cabezón D., Sanz J., Martí I., Van Beeck J., Sensitivity analysis of turbulence models in the ABL in Complex Terrain, Proceedings of the European Wind Energy Conference, May 2007, Milan (Italy)
10. Panofsky H., Dutton J., "Atmospheric Turbulence", Wiley, New York, 1984
11. Shih T., Liou W., et. al., A new  $k\epsilon$  eddy viscosity model for high Reynolds number turbulent flows, Journal of Computers Fluids, Vol. 24, pp. 227-238, 1995
12. Gómez-Elvira R., et.al., Anisotropy of turbulence in wind turbine wakes, J. Wind Engineering and Industrial Aerodynamics 93 (2005), 797-814
13. España G., Laporte L., Wind turbine wake characteristics in an Atmospheric Boundary Layer. Far Wake Physical and Numerical Modelling, Proceedings of EWEC 2008, Brussels (Belgium)